Chapter 11

Self-Organization of a Heteroditopic Molecule to Linear Polymolecular Arrays in Solution

11.1. Introduction

Nature displays a variety of supramolecular structures within a scale of 1 to 100 nm, beautifully put together with relatively simple building blocks by means of self-organization.[1-4] Complexes of great thermodynamic stability can form when there exist favorable complementary structural and electronic features at the recognition sites. Over the last few decades, chemists have elegantly adopted a variety of non-covalent bonding interactions to construct supramolecular architectures in the way that Nature does it.[5-11] Inspired by the versatility and efficiency of utilizing such non-covalent forces remarkably demonstrated in recent publications, we designed and prepared a heteroditopic molecule, containing complementary recognition sites of bis-*m*-phenylene crown ether and paraquat units,[12-19] to create linear oligo- and polymolecular arrays self-organized in solution by host-guest complexation. Each crown ether moiety in the structure accommodates the paraquat moiety of an adjacent unit to form non-covalently linked pseudo-oligomeric or pseudo-polymeric materials.[20,21]

11.2. Results and Discussion

11.2.1. Synthesis

The synthetic methodology employed for **3** from **1a**[22] and **2** is depicted in Figure 11.1. The synthesis of **2** was the first step toward preparation of the target heteroditopic molecule. Methyl iodide and 4,4'-bipyridine were stirred in a boiling solution of methanol and the product was precipitated out of the solution, driving the reaction equilibrium forward. The ^{1}H NMR spectrum of **2** in DMSO-d_6 after the ion exchange reaction revealed four sets of well separated doublet signals corresponding to the monopyridinium protons. The signal furthermost downfield at 9.11 ppm is assigned to

the protons adjacent to the electron deficient cationic site. The signals exhibited at higher field are due to the other three types of aromatic protons. The low yield (45%) may be explained in terms of **2** remaining in solution for a further reaction with excess of methyl iodide, giving the dipyridinium salt. In fact, the ^{1}H NMR spectrum of the crude product exhibits two sets of well resolved signals corresponding to the protons of the dipyridinium salt along with the four sets of doublets for **2**. Bromination of 5-hydroxymethylene bis(1, 3-phenylene)-32-crown-10 to obtain **1a** was initially carried out in acidic aqueous media with sodium bromide. Since the starting materials were left unreacted, an alternative synthetic path was sought. Bromination was eventually achieved using tribromophosphine in ethereal solution.[22] The first indication of the formation of **1a** was an upfield chemical shift of the resonance for the benzylic protons in the ^{1}H NMR spectrum. The shielding of the benzylic protons results from the substitution of –OH with less electronegative –Br. Further evidence of the successful bromination came from a sharp singlet resonance for the benzylic protons instead of the triplet observed for the starting material. A weak resonance at 4.94 ppm is attributed to the benzylic protons from inseparable quantity of the starting material after a number of recrystallizations.

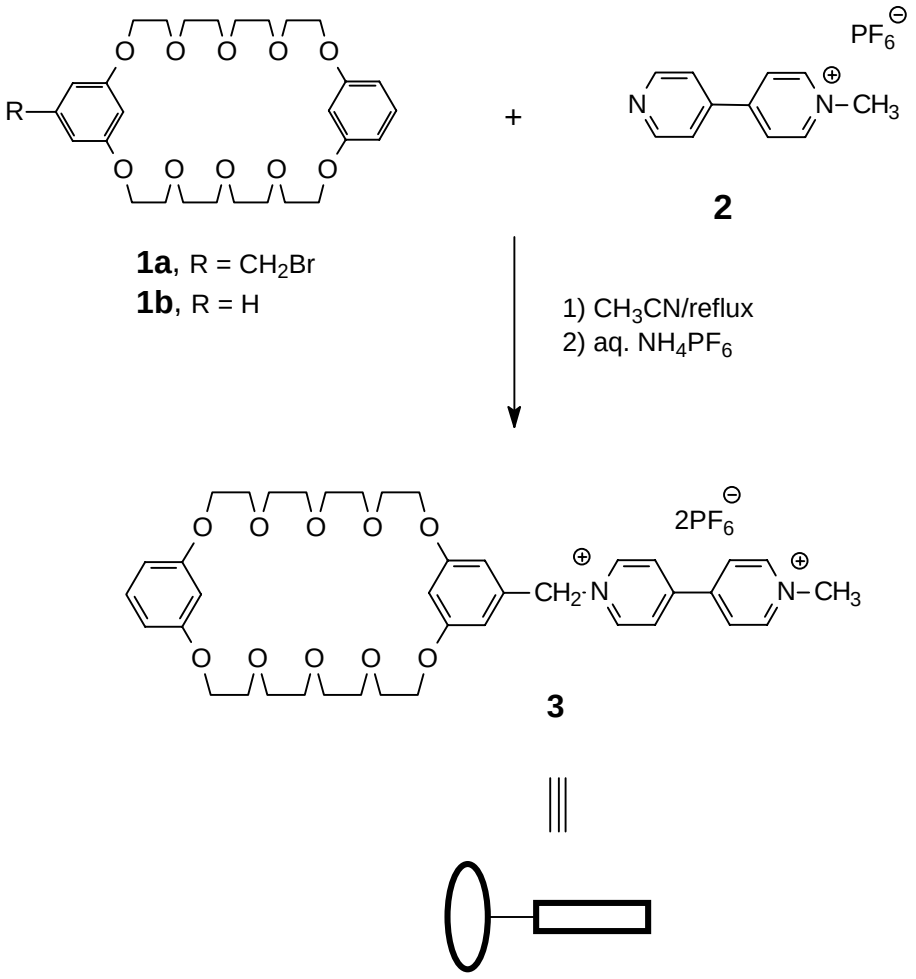

Figure 11.1. Synthesis of the heteroditopic molecule **3**.

To covalently bond the paraquat moiety to the crown ether, bromomethyl crown ether **1a** was reacted with 4-[4'-(*N*-methylpyridinium)]pyridine (**2**), followed by ion exchange to produce the heteroditopic molecule **3**. The ^{1}H NMR spectrum of **3** recorded in DMSO-d_6 is shown in Figure 11.2 and the signal assignments are given. In such a competitive solvent, the chemical signals corresponding to uncomplexed **3** can be observed. According to CPK models, the existence of the complex **4** was disregarded based on the stiffness of the molecule, which effectively prevents the paraquat unit from curling around to complex intramolecularly with the macrocyclic unit (Figure 11.3). Intermolecular complexation of **3** can lead to the formation of linearly chained, pseudo-polymeric supramolecules **5** as illustrated in Figure 11.3.

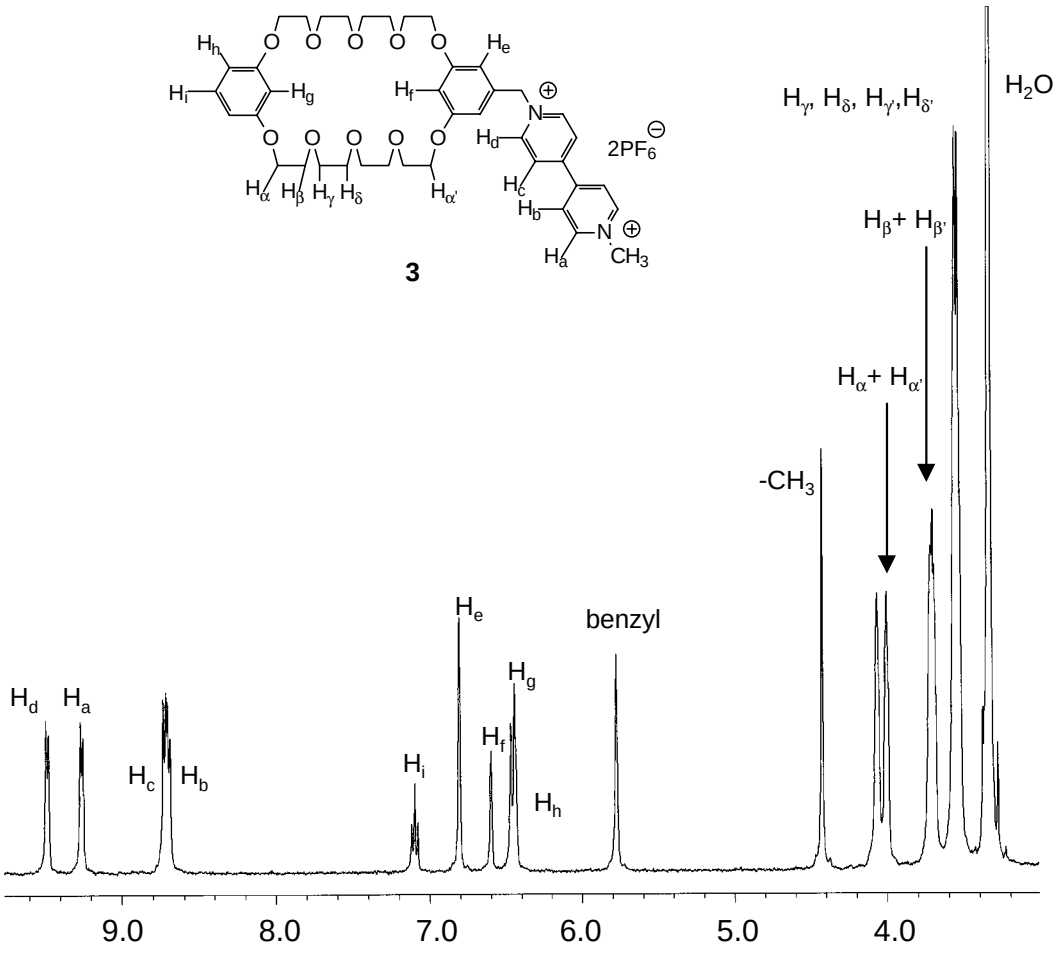

Figure 11.2. The ^{1}H NMR spectrum of **3** (400 MHz, DMSO-d_6, 22^{o}C).

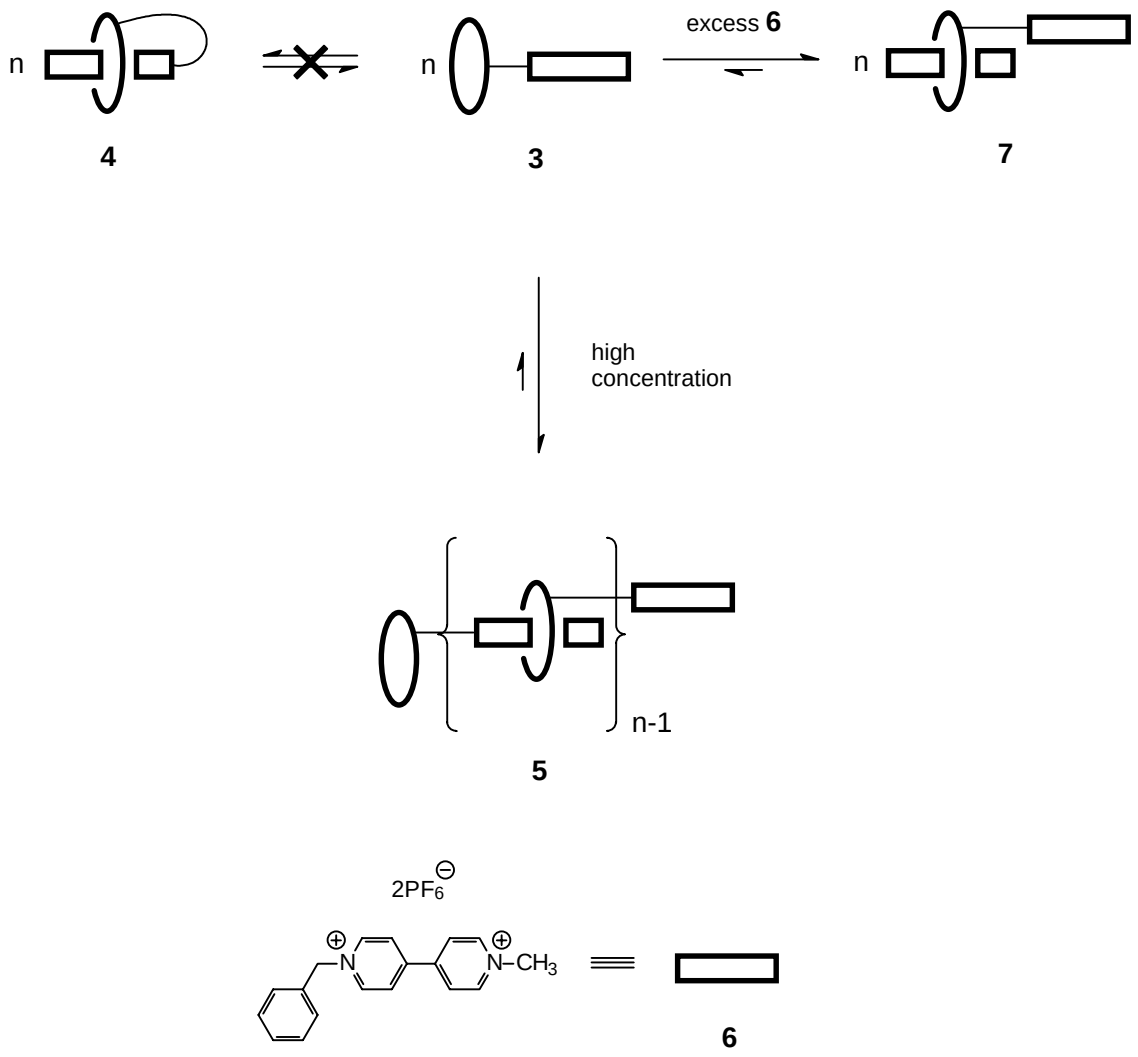

Figure 11.3. Illustration of the formation of the linear oligo- and polymolecular arrays **5** by self-organization of **3**.

11.2.2. Self-organization in solution

The ^{1}H NMR spectra of **3** in acetone-d_6 at 22^{o}C (Figure 11.4) are concentration dependent, reflecting the involvement of rapidly exchanging non-covalent bonding interaction(s) in solution. The chemical shift of a proton located in the cavity of the crown ether binding site, H_g, was monitored by ^{1}H NMR spectroscopy. The observed time averaged chemical shifts can be defined by using the chemical shifts obtained for totally complexed and free crown ether: $\delta_o=\delta_c p+\delta_u(1-p)$. δ_c is the chemical shift in a solution in which the crown ether is 100% complexed and δ_u is that of the free crown ether, and p is the fraction of the complexed crown ether. δ_u and δ_c were determined as

follows. The chemical shifts of H_g detected in the ^1H NMR spectra of the three most dilute solutions of **3** (6.5×10^{-5}, 3.1×10^{-5} and 1.6×10^{-5} M, acetone-d_6) were unchanged at 6.335 ppm. Thus, δ_u=6.335. A dilute solution of **3** (5.0×10^{-4} M, acetone-d_6) was gradually saturated with **6** which closely resembles the paraquat component of **3**, to emulate the binding sites of **5** by forming the heterodimeric **7** (Figure 11.3). The chemical shifts of H_g of **3** observed in the ^1H NMR spectra with the two most concentrated solutions of **6** (2.5×10^{-1} and 5.0×10^{-1} M, acetone-d_6) were unchanged at 5.825 ppm. This was taken as δ_c. Thus from δ_o, p was calculated. From p, one can estimate the average number of units in the aggregate **5** as follows: n=1/(1-p). Shown in Table 1 are n values calculated in this manner. As concentration increases the size of the aggregates increases to truly large values and non-covalently bonded polymers are formed. Since the molecular weight of **3** is 1,010 g/mole, for n=50 the total molar mass is 50,500 g/mole! Nearly identical results were obtained by analysis of the signal for H_f. It should be noted that the expression, n=1/(1-p), assumes that cyclic species do not contribute to consumption of host and guest sites. In covalent polymer chemistry it is well understood that the percentage of cyclic molecules of any size formed at high concentrations, *e.g.*, 1.0 M, is very small indeed (<3 %) and that linear macromolecules are preferentially formed.[23,24] Therefore, the validity of the assumption of the absence of cyclic complexes dramatically increases with concentration.

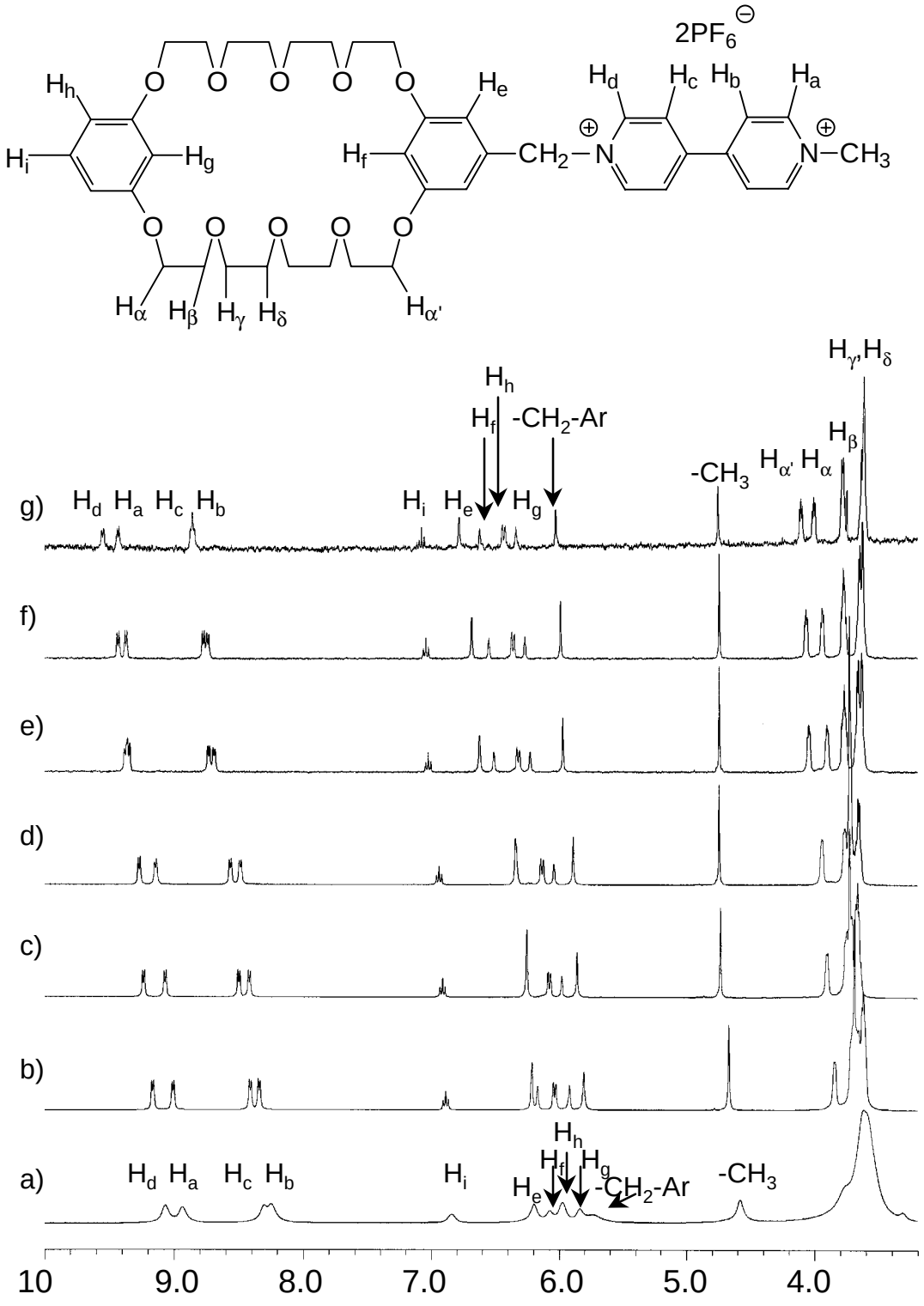

Figure 11.4. The stacked ^{1}H NMR spectra recorded for **3** at concentrations of a) 2.0, b) 5.0 x 10^{-1}, c) 5.0 x 10^{-2}, d)1.0 x 10^{-2}, e) 1.0 x 10^{-3}, f) 5.0 x 10^{-4}, and g) 6.3 x 10^{-5} M (400 MHz, acetone-d_6, 22^{o}C).

Table 11.1. Table of $[M]_0$, δ_o, p and n. δ_o values were obtained for H_g in the ^1H NMR spectra at corresponding concentrations of $[M]_0$ (400 MHz, acetone-d_6, 22°C)

$[M]_0$/M	δ_o/ppm	p	n
2.0	5.839	0.98	50
1.4	5.862	0.93	14
1.0	5.881	0.89	9.1
$5.0x10^{-1}$	5.918	0.82	5.6
$1.0x10^{-1}$	5.964	0.73	3.7
$6.7x10^{-2}$	5.974	0.71	3.4
$5.0x10^{-2}$	5.977	0.70	3.3
$1.0x10^{-2}$	6.041	0.58	2.4
$1.0x10^{-3}$	6.227	0.21	1.3
$5.0x10^{-4}$	6.268	0.13	1.1

The signal corresponding to the methyl group of the heteroditopic molecule in **5** is strongly shifted upfield (~0.2 ppm) at higher concentration (2.0 M in Figure 11.4a). Similarly, a significant upfield chemical shift is observed for the methyl group of **6** in the ^1H NMR spectrum of a 1:1 solution of monotopic components **1b** and **6** (acetone-d_6) at higher concentration, *e.g.*, 2.0 M each. These observations can be explained by the increased concentration of free PF_6^- in solution as the paraquat sites are complexed with the crown moieties. To demonstrate this experimentally, an acetone solution of **6** (1.0×10^{-2} M) was mixed with various concentrations of tetrabutylammonium hexafluorophosphate solutions (from 1.0×10^{-1} to 2.0 M) and the ^1H NMR spectra were obtained (Figure 11.5). The higher the concentration of PF_6^-, the greater the upfield chemical shift of the methyl group. On the other hand, the chemical shift of the phenyl group of **6** is independent of PF_6^- concentration. Therefore, the observed chemical shifts of H_g in Figure 11.4 are caused by complexation, not by the changes of PF_6^- concentration, validating the calculation of p and n based on the ^1H NMR data.

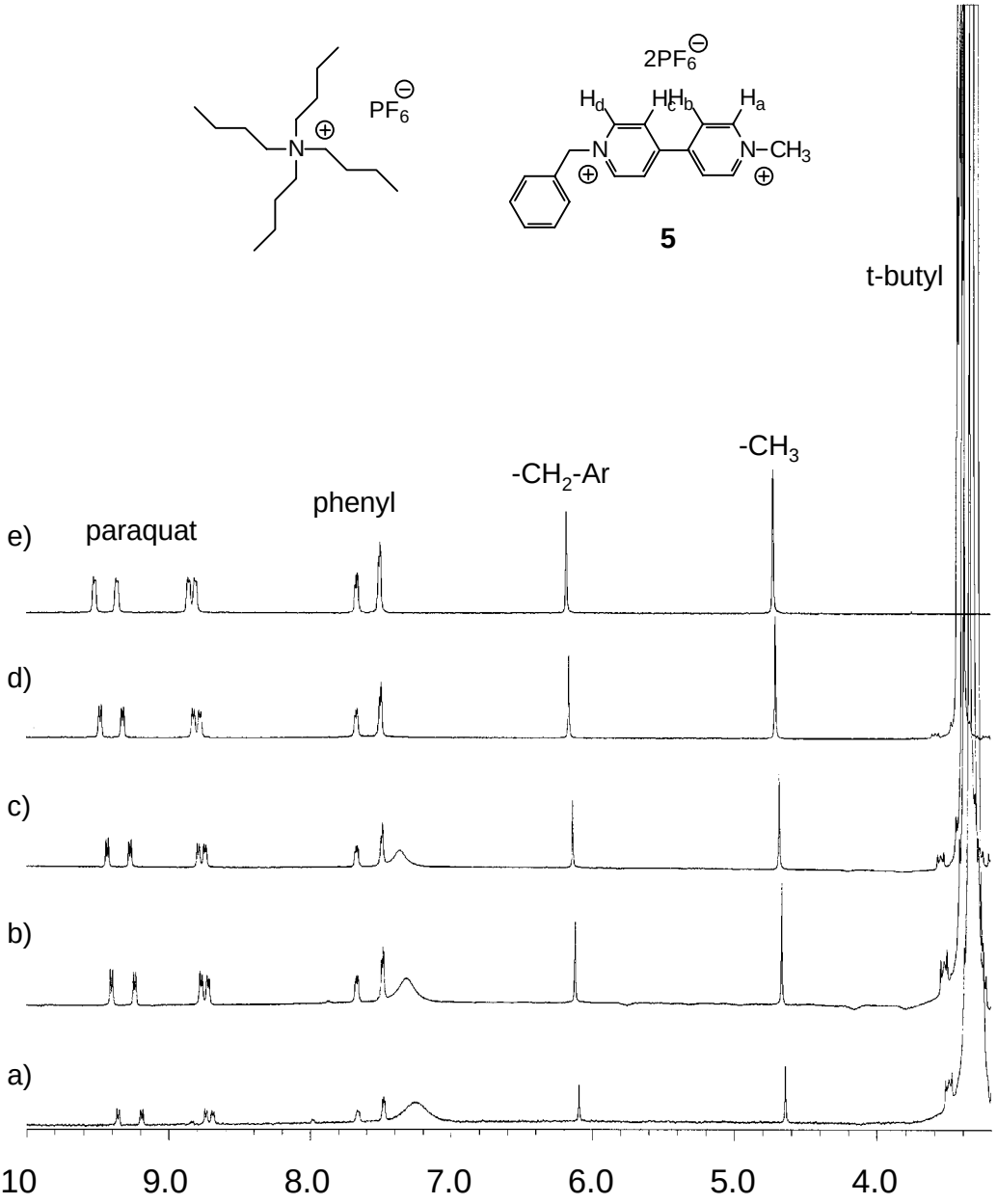

Figure 11.5. The stacked ^{1}H NMR spectra of a 1.0 x 10^{-2} M solution of **5** mixed with a) 0, b) 1.0 x10^{-1}, c) 5.0 x10^{-1}, d) 1.0, and e) 2.0 M solution of tetrabutyl ammonium hexafluorophosphate (400 MHz, acetone-d_6, 22^{o}C).

The ^{1}H NMR spectrum of **3** at 2.0 M (Figure 11.4a) clearly reveals signals substantially broadened with respect to the spectra recorded at lower concentrations. This can be understood in terms of the formation of larger pseudo-polymeric aggregates **5** at higher concentration; as a result the solution viscosity is increased (see below), and the

mobility of the polymeric chain is restricted, thus causing the signal broadening. In contrast, the ^{1}H NMR spectrum of a 1:1 solution of monotopic components **1b** and **6** in acetone (Figure 11.6) maintains sharp and well resolved signals even at the highest concentration we investigated (2.0 M/2.0 M). This observation, therefore, rules out non-ideality of highly concentrated solutions *per se* as a cause for the signal broadening.

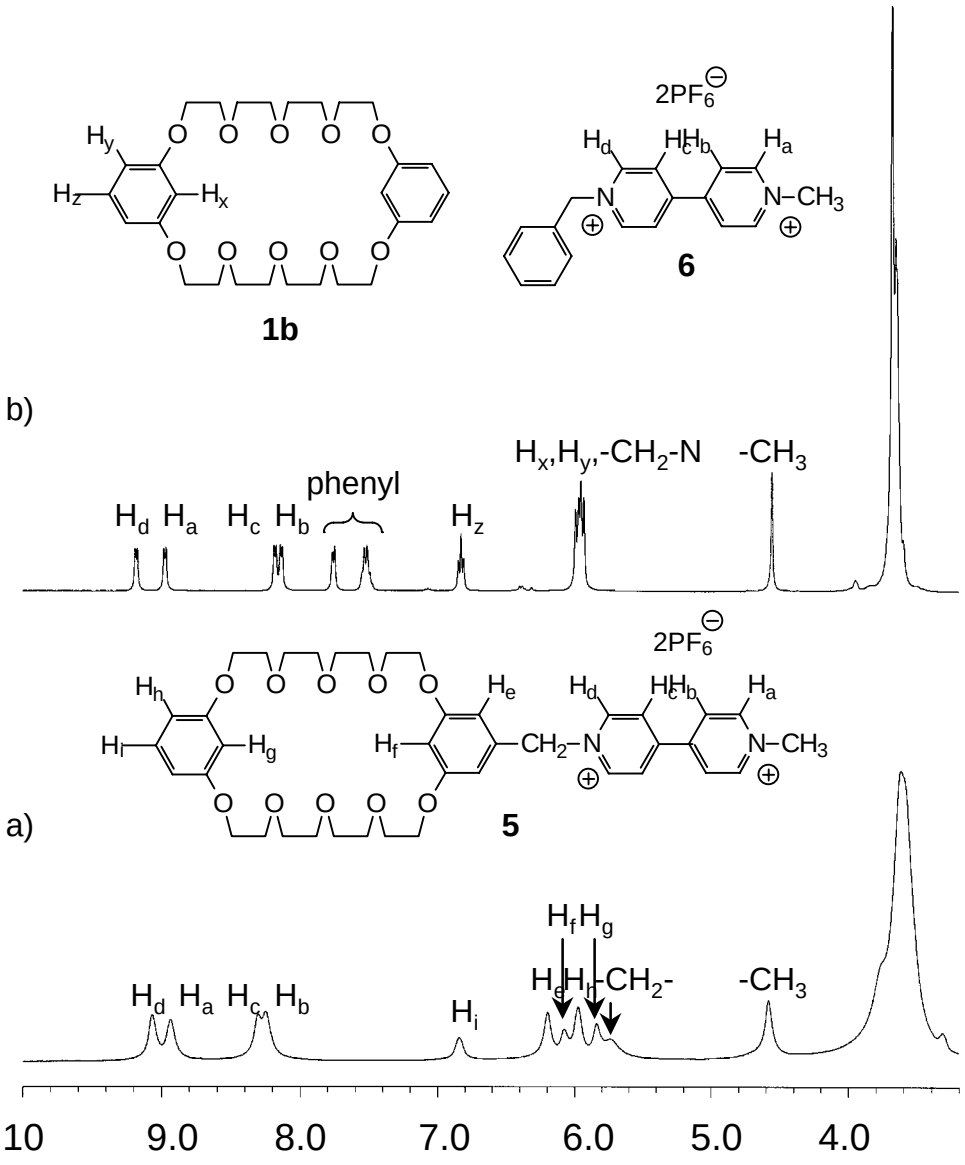

Figure 11.6. The ^{1}H NMR spectra of a) **5** at 2.0 M and b) **1b** and **6** (2.0/2.0 M) (400 MHz, acetone-d_6, 22^{o}C).

The 2D-NMR study (NOESY) was consistent with the pseudorotaxane geometry formed between the two complementary functionalities of adjacent units. The NOESY spectrum of a 5.0 x 10^{-1} M acetone-d_6 solution of **3** is shown in Figure 11.7. The NOESY spectra at higher concentrations could not be recorded because of overloading of the analog to digital converter. As expected, the ethyleneoxy protons, H_α, H_β, and H_γ, strongly interact through space with the protons of the paraquat unit (H_a-H_d) and also with the benzylic methylene protons. Most importantly, H_b and H_c of the paraquat moiety experience through space interactions with the aromatic protons residing inside the crown ether cavity, H_f and H_g, but not with those outside the cavity, H_e, H_h and H_i.

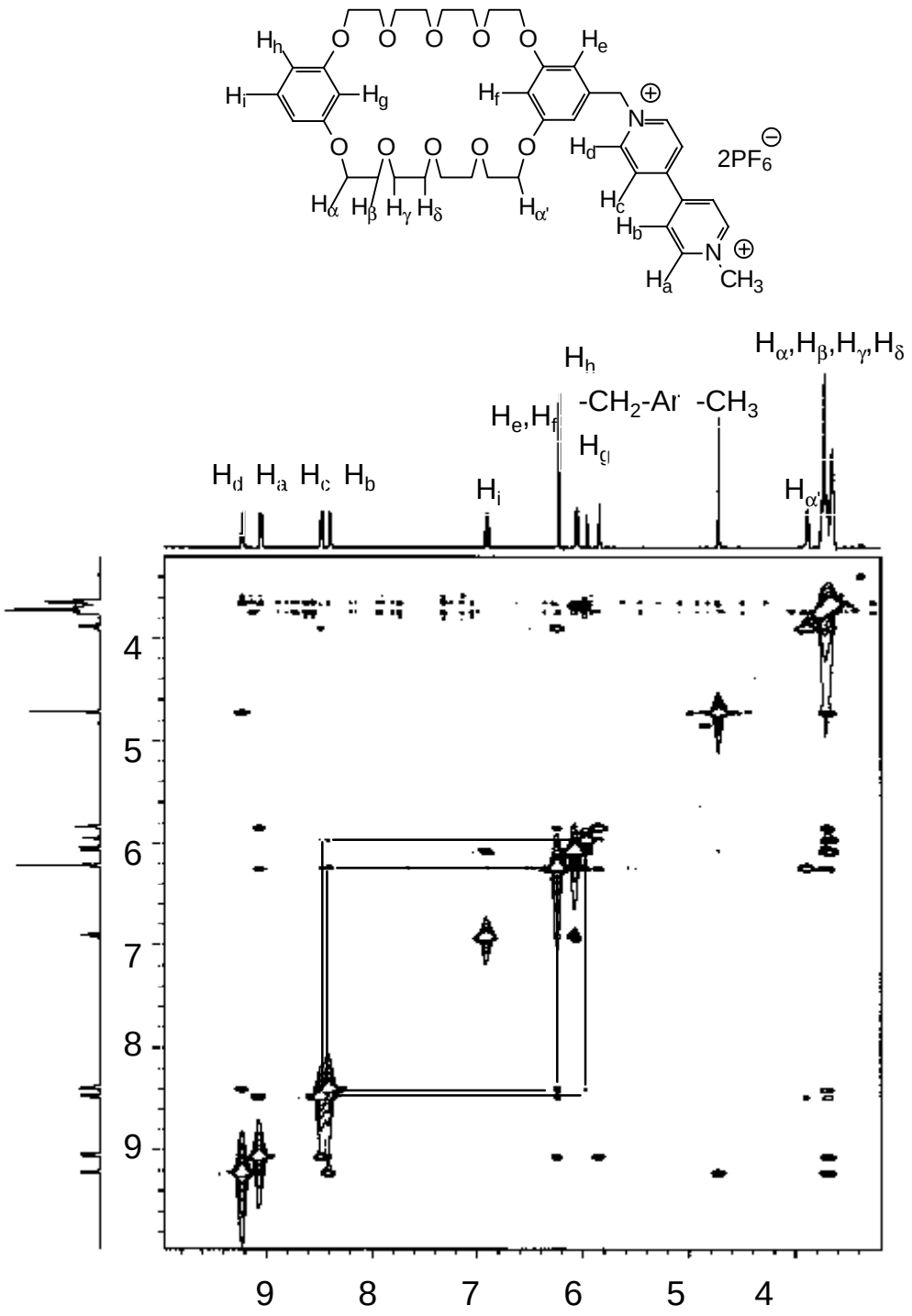

Figure 11.7. The NOESY spectrum of **5** (400 MHz, acetone-d_6, 30^{o}C).

High solution viscosity is characteristic of linear polymeric structures. Indeed, the reduced viscosity of acetone solutions of **3** increased in non-linear fashion with

concentration due to the formation of **5** (Figure 11.8a) while that of equimolar acetone solutions of **1b** and **6** increased only slightly with concentration (Figure 11.8b), thus ruling out the polyelectrolyte effect as the major cause of the viscosity change observed with **5**. The high viscosity observed for **5** at 1.4 M (n=14 from Table 1), η_{red}=0.26 vs. 0.13 dL/g for 1:1 of **1b**:**6**, and the fact that a 2.0 M acetone solution of **5** was too viscous to flow through the viscometer argue against the presence of significant amounts of small cyclic species, since it is well known that cyclic molecules have smaller hydrodynamic volumes and hence lower viscosities than their linear counterparts.[25,26]

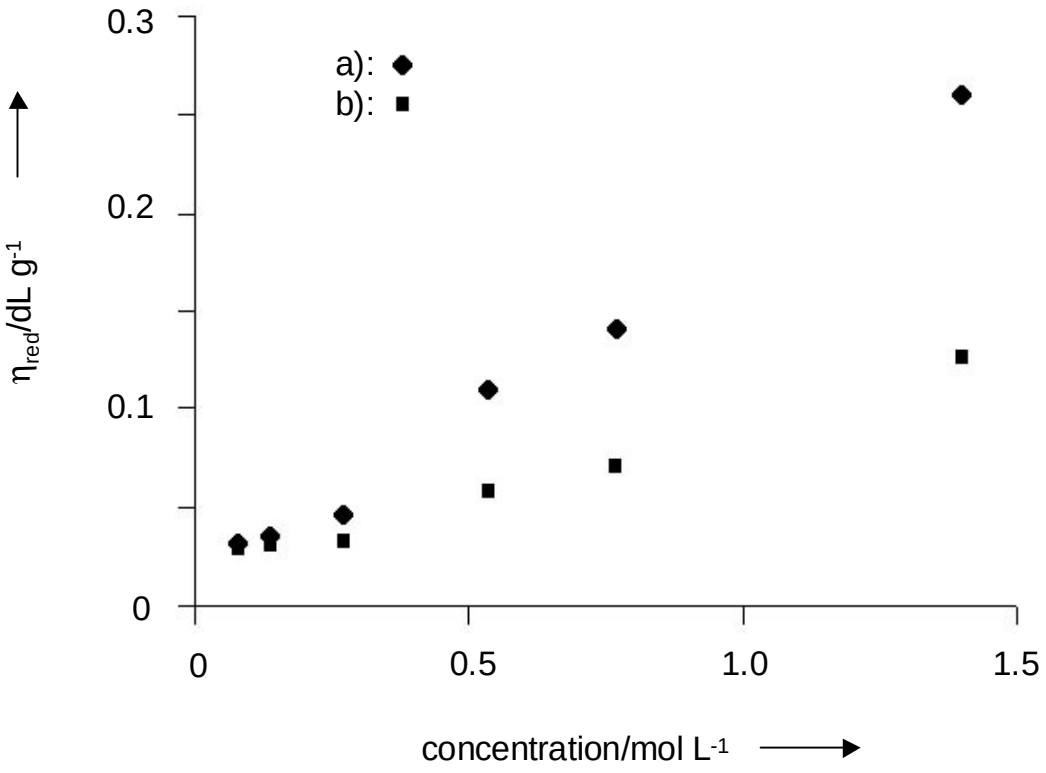

Figure 11.8. Reduced viscosity as a function of concentration (solutions in acetone at 22^{o}C) a) **5** and b) **1b** and **6** (1:1).

11.2.3. Characterization of linear arrays in the solid state

Thermal analyses of **5** were conducted by DSC. Two samples of red-orange colored *amorphous* **5** prepared by freeze-drying 1.0 x 10^{-1} and 1.0 M acetone solutions of

the heteroditopic molecule **3** exhibited glass transitions (T_g) at 42.1 and 58.3^{o}C, respectively. On the other hand, **3**, recrystallized from water, in which self-organization does not occur, is *crystalline* and displays a melting transition at 80.3^{o}C. The amorphous nature of the samples prepared in acetone is indicative of linear polymers. Furthermore, the higher T_g observed for **5** obtained from the 1.0 M solution relative to the 1.0 x 10^{-1} M material is consistent with a higher extent of self-organization, n, as demonstrated by the ^{1}H NMR and viscosity experiments. The ^{1}H NMR spectra of 1.0 x 10^{-1} and 1.0 M acetone solutions at lower temperatures revealed that the chemical shifts of H_g observed at –20^{o}C down to slightly above the freezing temperature of the solvent (-94^{o}C) were unchanged at 5.944 and 5.862 ppm, which correspond to n values of 4.3 and 14, respectively.

Mass spectrometry was utilized to support the existence of the self-organized linear arrays. The spectrum was immediately recorded in the positive ion mode after a 5.0 x 10^{-1} M acetone solution of **5** (n=5.6 from Table 11.1) was mixed with the matrix (3-nitrobenzyl alcohol) on the probe. The FAB mass spectrum (Figure 11.9) reveals peaks at *m/z*=3896 and 3751, corresponding to the tetramer **5**, n=4 after the loss of one and two PF_6 units, respectively. The peaks at *m/z*=2886 and 2741 indicate the existence of trimeric oligomer **5**, n=3 after the successive loss of one and two PF_6 units, respectively. In addition, we observed the $[M_2\text{-}PF_6]^+$, $[M_2\text{-}2PF_6]^+$, $[M\text{-}PF_6]^+$ and $[M\text{-}2PF_6]^+$ peaks, corresponding to the dimeric and monomeric species. The relative heights for the $[M_4\text{-}PF_6]^+$, $[M_3\text{-}PF_6]^+$ and $[M_2\text{-}PF_6]^+$ peaks were 0.29, 1.4 and 22% of the base peak $[M\text{-}PF_6]^+$, respectively.

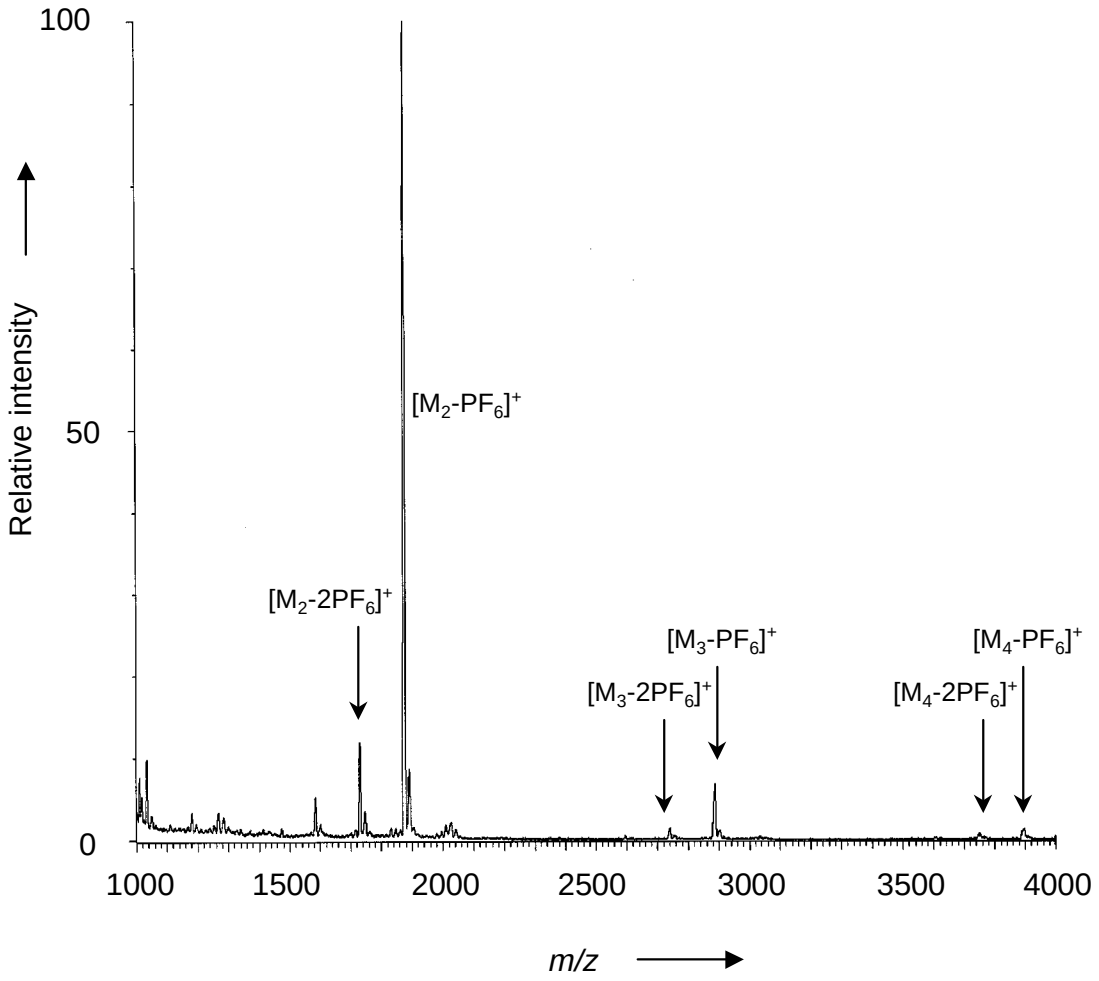

Figure 11.9. The FAB mass spectrum of the self-organized pseudo-oligomeric material **5**.

Not surprisingly, fibers were pulled from a concentrated acetone solution (>2.0 M). The scanning electron microscope (SEM) images of ribbon-like fibers with 10-15 μm in width are shown in Figure 11.10. The fiber formation is indicative of significant linear array extension in the material, consequently giving rise to polymeric properties, since macromolecular entanglements are required to produce such fibers, since macromolecular entanglements are required to produce such fibers. The atomic force microscope (AFM) images of the fibers revealed that the surface of these fibers are considerably smooth (Figures11.11 and 11.12).

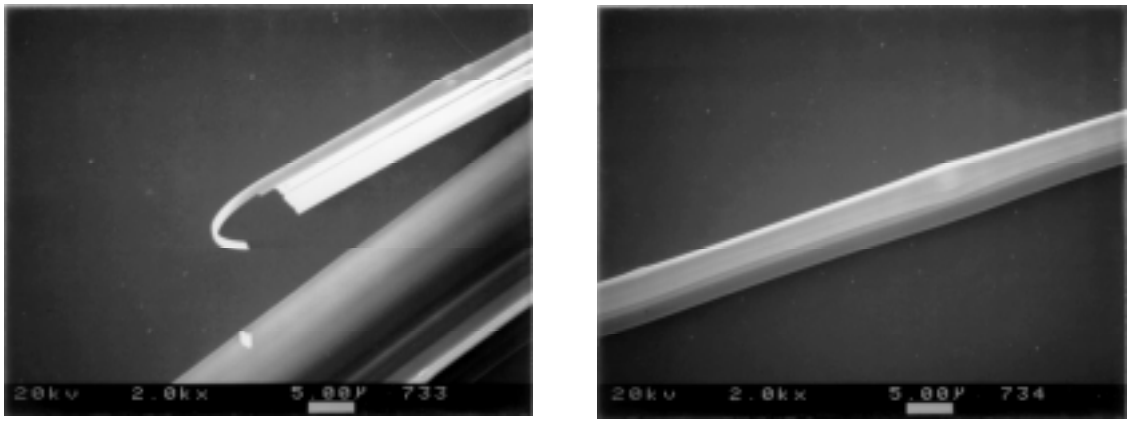

Figure 11.10. Longitudinal views of scanning electron micrographs of a fiber pulled from a concentrated acetone solution of **3** (>2.0 M).

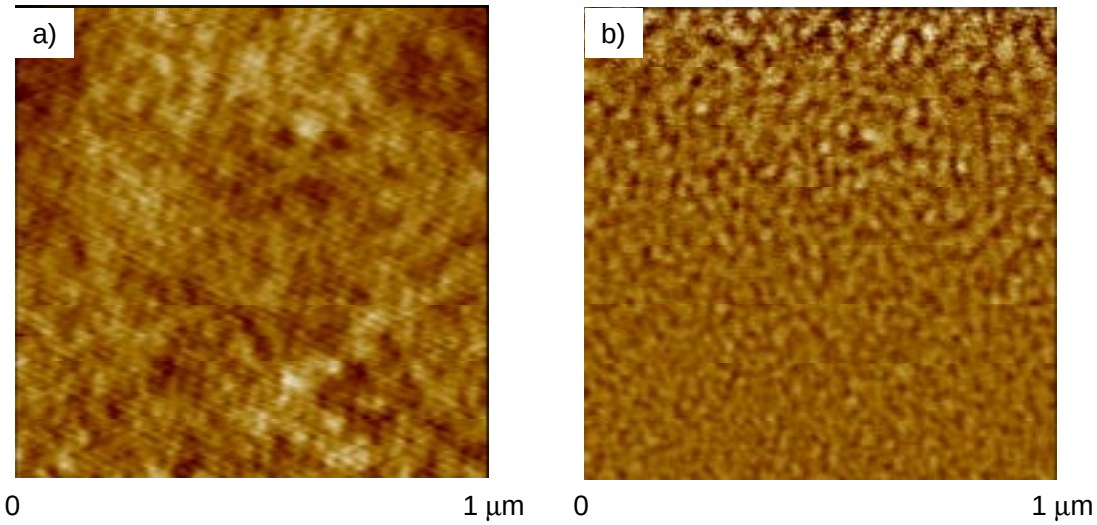

Figure 11.11. The AFM images of a fiber pulled from a concentrated acetone solution of **3** (>2.0 M) a) height and b) phase.

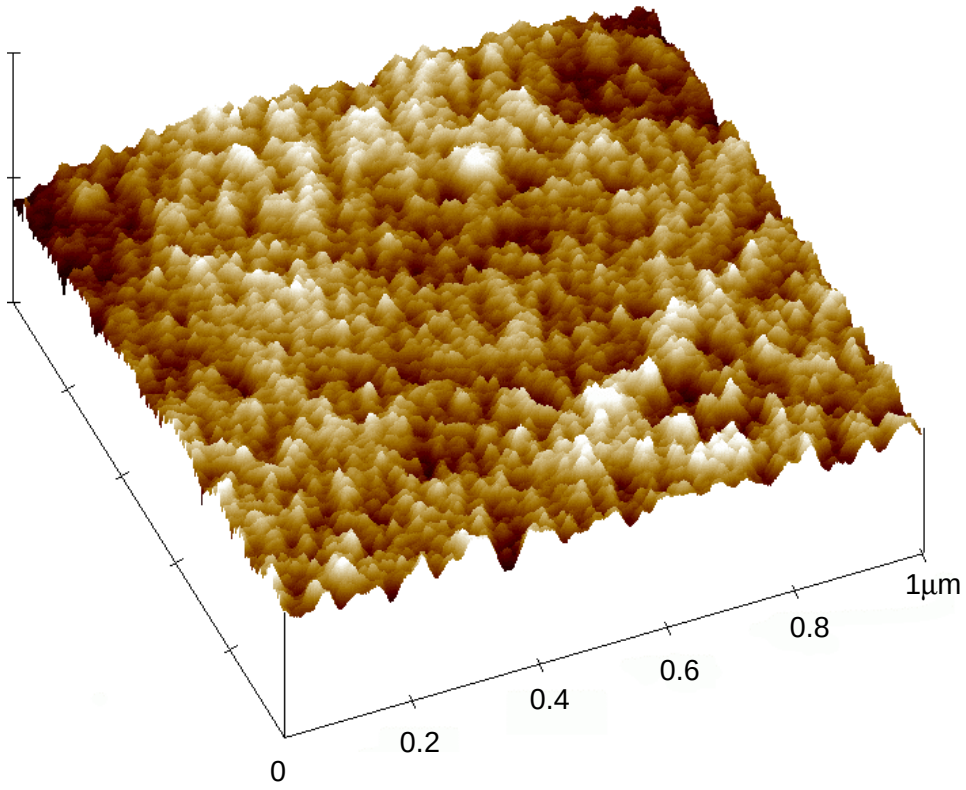

Figure 11.12. Roughness analysis of the fiber surface.

11.3. Conclusion

We demonstrated that the heteroditopic molecule **3** instantaneously "self-associated" to form pseudo-oligomeric and pseudo-polymeric rotaxane types of linear arrays in solution. The trapping of the crown ether moieties in such linear arrays **5** by the use of blocking chemistry will lead to mechanically "locked-in" linear arrays which may ultimately be studied by using other characterization techniques available in polymer science. This exciting concept of utilizing non-covalent bonding interactions can potentially be expanded to achieve other novel self-organizing nanoscopic structures; we are pursuing such objectives.

11.4. Experimental

THF was distilled from Na and benzophenone. All other solvents were used as received. Melting points were taken on a Mel-Temp II melting point apparatus and are uncorrected. The 400 MHz ^{1}H NMR spectra were recorded on a Varian Unity with

tetramethylsilane (TMS) as an internal standard. The following abbreviations are used to denote splitting patterns: s (singlet), d (doublet), t (triplet), and m (multiplet). Differential scanning calorimetry (DSC) was performed on a Perkin-Elmer Series-4 calorimeter under a nitrogen purge using indium as the calibration standard. Scanning electron microscopy (SEM) was performed on a Philips 420T. The copper substrate was sputtered with gold after sample deposition and before exposure to the electron beam. Elemental analyses were obtained from Atlantic Microlab, Norcross, GA. Mass spectra were provided by the Washington University Mass Spectrometry Resource, an NIH Research Resource (Grant No. P41RR0954).

5-Bromomethyl-1,3-phenylene-*m*-phenylene-32-crown-10 (1a). To a 250 mL round bottom flask equipped with a magnetic stirrer and N_2 inlet were added 5-hydroxymethylene-1,3-phenylene-*m*-phenylene-32-crown-10 (0.69 g, 1.2 mmol) and a mixture of toluene and diethyl ether (130/30 mL). To this solution was added tribromophosphine (1 mL) and the reaction mixture was vigorously stirred for 18 h at 25^{o}C. The reaction was quenched with a small amount of H_2O. The solvents were removed *in vacuo* and the resulting crude product was suspended in H_2O and extracted with $CHCl_3$. The organic layers were combined, dried over $MgSO_4$, and concentrated to give a colorless liquid, which was subsequently recrystallized from EtOH to afford a white solid (0.72 g, 94% yield), mp 64-65^{o}C (lit. mp 63.7-65.4^{o}C). ^{1}H NMR (400 MHz, DMSO-d_6, 22 °C): δ=3.54 (16H, m), 3.69 (8H, m), 4.02 (8H, m), 4.56 (2H, s), 6.45-6.57 (6H, m), and 7.11 (1H, t, J = 3.2 Hz).

4-[4'-(*N*-methylpyridinium)]pyridine hexafluorophosphate (2). To a 250 mL round bottom flask equipped with a magnetic stirrer and a condenser were added 4,4'-bipyridine (10.0 g, 64.2 mmol) and MeOH (80 mL) and the solution was warmed to 40^{o}C. To this solution was added a solution of methyl iodide (10.8 g, 76.2 mmol) in MeOH (5 mL) dropwise and the reaction mixture was vigorously stirred under reflux for 24 h. The reaction mixture was cooled to 0^{o}C and the orange precipitate was filtered. The crude product was boiled in $CHCl_3$ and the suspended materials were filtered to give an orange

solid, which was subsequently recrystallized from a mixture of MeOH and $CHCl_3$ to afford a yellow solid (8.66 g, 45% yield), mp decomp. 330°C. This product was used in the next step without further purification. To a 250 mL round bottom flask equipped with a magnetic stirrer were added 4-[4'-(*N*-methylpyridinium)]pyridine iodide (8.66 g, 29.0 mmol) and H_2O (100 mL). To this solution was added aq. NH_4PF_6 until no further precipitation was observed. The precipitate was filtered and recrystallized from H_2O to afford a white solid (6.77 g, 73% yield), mp 219-220°C. ^{1}H NMR (400 MHz, DMSO-d_6, 22 °C): δ=4.36 (3H, s), 8.02 (2H, d, *J* = 6.4 Hz), 8.59 (2H, d, *J* = 6.4 Hz), 8.85 (2H, d, *J* = 6.4 Hz), and 9.11 (2H, d, *J* = 6.4 Hz).

***N*-methyl-*N'*-[5-methylene bis(1,3-phenylene)-32-crown-10]-4,4'-bipyridine bis(hexafluorophosphate) (3).** In a 50 mL round bottom flask equipped with a magnetic stirrer **1b** (0.35 g, 0.56 mmol), **2** (0.18 g, 0.57 mmol) and MeCN (20 mL) were refluxed 24 h. The orange solution was precipitated in Et_2O to afford a yellow solid which was dissolved in H_2O and aq. NH_4PF_6 was added until no further precipitation was observed. The product was recrystallized from H_2O to give a yellow solid (0.50 g, 89 % yield), mp 79-80°C. ^{1}H NMR (400 MHz, DMSO-d_6, 22°C): δ=3.55 (16H, m), 3.70 (8H, t, *J* = 3.2 Hz), 4.00 (4H, t, *J* = 3.2 Hz), 4.07 (4H, t, *J* = 3.2 Hz), 4.21 (3H, s), 5.77 (2H, s), 6.44-6.47 (3H, m), 6.60 (1H, s), 6.80 (2H, s), 7.10 (1H, t, *J* = 3.6 Hz), 8.69 (2H, d, *J* = 6.4 Hz), 8.72 (2H, d, *J* = 6.4 Hz), 9.25, (2H, d, *J* = 6.4 Hz), and 9.48(2H, d, *J* = 6.4 Hz). Anal. Calcd for $C_{40}H_{52}N_2O_{10}P_2F_{12}$: C, 47.63; H, 5.00. Found: C, 47.35; H, 5.02.

11.5. References

1)Klug, A. *Angew. Chem. Int. Ed. Engl.* **1983**, *22*, 565-582.

2)Philp, D.; Stoddart, J. F. *Angew. Chem. Int. Ed. Engl.* **1996**, *35*, 1154-1196.

3)Whitesides, G. M.; Mathias, J. P.; Seto, C. T. *Science* **1991**, *254*, 1312-1319.

4)Lindsey, J. S. *New J. Chem.* **1991**, *15*, 153-180.

5)Harada, A.; Li, J.; Kamachi, M. *Nature* **1992**, *356*, 325-327.

6)Harada, A.; Li, K.; Kamachi, M. *Nature* **1994**, *370*, 126-128.

7)Seto, C. T.; Whitesides, G. M. *J. Am. Chem. Soc.* **1993**, *115*, 905-916.

8)Whitesides, G. M.; Ismagilov, R. F. *Science* **1999**, *284*, 89-92.

9)Lehn, J.-M. *Supramolecular Chemistry Concepts and Perspectives*; VCH: New York, 1995.

10)Lehn, J.-M. *Makromol. Chem., Macromol. Symp.* **1993**, *69*, 1-17.

11)Lehn, J.-M. *Angew. Chem. Int. Ed. Engl.* **1990**, *29*, 1304-1319.

12)Allwood, B. L.; Shahriari-Zavareh, H.; Stoddart, J. F.; Williams, D. J. *J. Chem. Soc., Chem. Commun.* **1987**, 1058-1061.

13)Asakawa, M.; Ashton, P. R.; Ballardini, R.; Balzani, V.; Belloharadský, M.; Gandolfi, T.; Kocian, O.; Prodi, L.; Raymo, F. M.; Stoddart, J. F.; Venturi, M. *J. Am. Chem. Soc.* **1997**, *119*, 302-310.

14)Ashton, P. R.; Philp, D.; Reddington, M. V.; Slawin, A. M. Z.; Spencer, N.; Stoddart, J. F.; Williams, D. J. *J. Chem. Soc., Chem. Commun.* **1991**, 1680-1683.

15)Ashton, P. R.; Parsons, I. W.; Raymo, F. M.; Stoddart, J. F.; White, A. J. P.; Williams, D. J.; Wolf, R. *Angew. Chem. Int. Ed.* **1998**, *37*, 1913-1916.

16)Amabilino, D. B.; Stoddart, J. F. *Chem. Rev.* **1995**, *95*, 2715-2828.

17)Amabilino, D. B.; Ashton, P. R.; Balzani, V.; Brown, C. L.; Credi, A.; Fréchet, J. M. J.; Leon, J. W.; Raymo, F. M.; Spencer, N.; Stoddart, J. F.; Venturi, M. *J. Am. Chem. Soc.* **1996**, *118*, 12012-12020.

18)Amabilino, D. B.; Ashton, P. R.; Boyd, S. E.; Gómez-López, M.; Hayes, W.; Stoddart, J. F. *J. Org. Chem* **1997**, *62*, 3062-3075.

19)Raymo, F. M.; Houk, K. N.; Stoddart, J. F. *J. Am. Chem. Soc.* **1998**, *120*, 9318-9322.

20)Hirotsu, K.; Higuchi, T.; Fujita, K.; Uedo, T.; Shinoda, A.; Tabushi, I. *J. Org. Chem.* **1982**, *47*, 1143-1144.

21)Helgeson, R. C.; Tarnowski, T. L.; Timko, J. M.; Cram, D. J. *J. Am. Chem. Soc.* **1977**, *99*, 6411-6418.

22)Gibson, H. W.; Nagvekar, D. S.; Yamaguchi, N.; Wang, F.; Bryant, W. S. *J. Org. Chem.* **1997**, *62*, 4798-4803.

23)Hamilton, S. C.; Semlyen, J. A. *Polymer* **1997**, *38*, 1685-1691.

24)Odian, G. *Principles of Polymerization*; Third Edition ed.; John Wiley & Sons, Inc.: New York, 1991.

25)Dodgson, K.; Semlyen, J. A. *Polymer* **1977**, *18*, 1265-1268.

26)Hild, G.; Strazielle, C.; Rempp, P. *Eur. Polym. J.* **1983**, *19*, 721-727.